RESEARCH PAPER

Formulation and Evaluation of Curcumin-Loaded Leciplex for Enhanced Antifungal Activity Against Candidiasis

Prafulla Chaudhari[1*], Priyanka Chaudhari[2], Ashlesha Pandit[1], Rohini Kolhe[1], Manisha Khaire[2], Nikita Shinde[1], Suvarna A.Vadje[3]

1. JSPMs Rajarshi Shahu College of Pharmacy and Research, Tathawade, Pune -411033, Maharashtra, India.
2. S.J.V.P. M's, Rasiklal M. Dhariwal Institute of Pharmaceutical Education & Research, D2 60-61, Telco Road, Chinchwad Station, Pune- 411019, Maharashtra, India.
3. PES's Modern College of Pharmacy, Nigdi, Pune

[*]**Corresponding author: Dr. Prafulla S. Chaudhari**
*Associate Professor Department of Pharmaceutics, JSPM's Rajarshi Shahu College of Pharmacy and Research, Tathawade, Pune, 411033, Maharashtra, India. E-mail Id: Praful.pharma@gmail.com

Abstract

Objective

Every year, fungal diseases claim the lives of over 3.75 million people worldwide, and the lack of effective treatments and the emergence of medication resistance are significant obstacles. The natural substance curcumin, which has strong antibacterial qualities, has a low bioavailability.

Methods

Curcumin loaded leciplex formulated by simple one step creation technique using phospholipid, CTAB and transcutol HP. The prepared leciplex were optimized through custom design. Formulation integrated into Carbopol gel system and assessed for various parameter such as mean particle size, PDI, entrapment efficiency, zeta potential, in-vitro drug release and EX-vivo permeation.

Results

The optimized CUR–LP formulation exhibited a particle size of ~206.6 nm, PDI of 0.418, high entrapment efficiency (92.81 ± 1.02%), and a positive zeta potential (+26.30 mV), indicating good stability and enhanced skin adhesion. DSC and SEM analyses confirmed successful incorporation of curcumin into uniformly distributed spherical nanoparticles. The CUR–LPG gel showed suitable physicochemical properties, including a skin-compatible pH (5.64 ± 0.1), good spreadability, and appropriate mechanical strength for topical application. In vitro and ex vivo studies demonstrated sustained drug release and controlled skin permeation compared with CUR–LP and the marketed formulation. Furthermore, CUR–LPG exhibited superior antifungal activity against *Candida albicans*, with the highest zone of inhibition (24.1 ± 0.6 mm), highlighting its potential as an effective topical delivery system for prolonged antifungal therapy.

Conclusion

Overall, the results support the potential of CUR–LPG as a promising and effective topical therapy for fungal infections, offering enhanced stability, extended drug release, and improved therapeutic efficacy.

Graphical Abstract

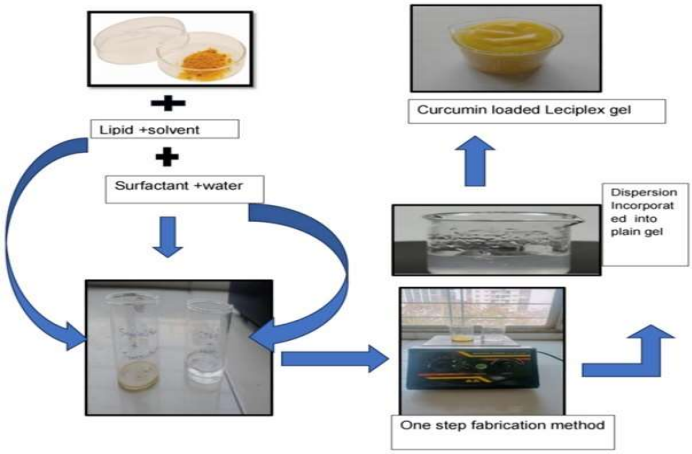

Keywords: Curcumin, antifungal, CTAB, candida albicans, leciplex.

*Author for Correspondence: Praful.pharma@gmail.com

How to cite this article: Chaudhari P, Chaudhari P, Pandit A, Kolhe R, Khaire M, Shinde N, Vadje SA. Formulation and Evaluation of Curcumin-Loaded Leciplex for Enhanced Antifungal Activity Against Candidiasis. Int J Drug Deliv Technol. 2026;16(69s):499-514. DOI: 10.25258/ijddt.16.69s.56

INTRODUCTION

Recent studies suggest that fungal diseases are responsible for around 3.75 million deaths globally each year — nearly twice the earlier estimates of 1.5 to 2 million annual deaths. Of these, approximately 68% (about 2.5 million) are directly caused by fungal infections[1]. Individuals with weakened immune systems are more prone to developing fungal infections, which can occur on various parts of the body. Common examples include onychomycosis and candidiasis. Certain fungal infections are linked to high mortality rates due to their severity and difficulty in treatment[2]. Fungal infections can range from gentle, facile conditions affecting the skin to severe, life-threatening systemic illnesses. Current antifungal treatments are confined to a few drug classes with many medications specifically targeting limited fungal species like *Candida*, *Aspergillus*, and *Cryptococcus*. Although these treatments can be effective, their use is often restricted due to issues such as toxicity, interactions with other drugs, suboptimal therapeutic outcomes, and rising antifungal resistance — especially in strains like *Candida auris* and *Aspergillus fumigatus*. These challenges emphasize the need for the modification of novel antifungal factor[3].

Curcumin, that is present in nature fall out under lipophilic polyphenolic compound[4]. The primary component of *Curcuma longa* is its rhizome, which contains a small, lipophilic molecule capable of easily penetrating cell membranes[5]. Curcumin's therapeutic utility is limited by its poor aqueous solubility, low gastrointestinal absorption, and rapid metabolic degradation, which collectively reduce its systemic bioavailability and hinder effective clinical outcomes [6]Research has demonstrated that curcumin have a wide range of biological activities, including blood sugar-lowering, antimicrobial, antiviral, neuroprotective, anti-inflammatory, anticancer, properties[7]. Minimizing the particle size of curcumin is essential for improving its pharmacological efficacy and bioavailability[8]. Nanotechnology enhances drug delivery, solubility, targeting, and exhibits direct antifungal effects by fungal cell disruption. However, clinical translation faces challenges like safety, toxicity, scalability, and controlled drug release [9, 10].

Liposomes, composed of phospholipid bilayers, have been widely studied as carriers for transdermal drug delivery[11,12]. Liposomes can encapsulate both hydrophilic and hydrophobic formed by combining anionic phospholipids with cationic surfactants[13]. Leciplex, prepared via a one-step fabrication process, carry a positive charge that enhances drug penetration by interacting with the negatively charged skin[14].

Hydrogels are three-dimensional structures formed by hydrophilic polymers[15] which contains chemical or physical cross-linking Carbopol®[16], and also biocompatible with the dermal cells[17,18]. Carbomer polymers have a cross-linked microgel network, which makes them highly suitable for use in dermatological drug delivery systems. The research study describes Curcumin-loaded Leciplex was successfully formulated and incorporated into a Carbopol-based hydrogel[19]. The optimized system showed improved drug release, skin permeability, and enhanced antifungal activity, indicating its potential as an effective topical antifungal treatment.

MATERIALS AND METHODS

Materials

Curcumin obtained from Herbo Nutra Pvt. Ltd (India). Transcutol® HP was acquired from Gattefossé, Saint-Priest, France. Cetyl trimethyl Ammonium bromide (CTAB) was purchased from Sisco Research Laboratories (Mumbai, India). Soybean Lecithin (Phospholipon® 90G, PL-90G) was an Otto Chemie Pvt Ltd. The Carbopol 940 was obtained from Lubrizol I Private Limited, (Mumbai). Dialysis membrane (Mol. Weight cut off 12000 – 14000) was obtained from, Hi-Media Laboratories (Mumbai). The culture of Candida albicans was received from National Centre for Microbial Resource (Pune). The Agar-Agar media were got from Research-lab Fine Chem Industries, (Mumbai, India). All remaining ingredients utilized of analytical grades.

Pre-formulation studies

Solubility study

To evaluate the solubility of curcumin, an excess amount of curcumin was added separately to (PBS, pH 6.8), distilled water, ethanol. Each mixture subjected to continuous agitation at 75 rpm using a shaker incubator maintained at 37 ± 0.5 °C for 48 hours to ensure equilibrium. Later on, incubation, samples centrifuged at 10,000 rpm for fifteen minutes to separate undissolved curcumin. The resulting supernatant was collected and analyzed spectrophotometrically to determine the concentration of solubilized curcumin.

UV spectrophotometric analysis of drug in various solvents

In ethanol

Stock solution initially processed by dissolving 10 mg drug in 100 mL of ethanol, yielding a concentration of 100 µg/ml. From primary solution, dilutions were prepared (1 µg/mL to 9 µg/ml). Readings of these diluted samples were UV spectrophotometrically calculated at 425 nm[20].

In phosphate buffer (PBS) 6.8

Preparation of curcumin stock solution involved solubilizing 10 mg of curcumin in 100 mL of PBS solution with a resulting concentration of 100 µg/mL were formulated using a pH 6.8 PBS containing 1.5% polysorbate 80. Subsequently, 5 µg/mL working solutions were prepared media. UV–Visible spectrophotometric analysis was carried out using the corresponding solvent systems as blanks, to identify the maximum absorbance wavelength (λmax) of curcumin. Figure represents the concentration versus absorbance data phosphate buffer at pH 6.8[21].

FTIR Studies

The FTIR spectrum of Curcumin, Physical mixture, Transcutol HP and CTAB were recorded across a range of 4000–400 cm^{-1}, with resolution of 2 cm^{-1} using FTIR Spectrophotometer (Brucker)[22]

Preparation of Curcumin Loaded Leciplex (CUR - LP)

The formation of lecithin-based cationic nanoparticles was done using a simple one-step production procedure. In short, 180 mg of soybean lecithin (Lipoid S 100) and 90 mg of CTAB were carefully weighed and then transferred to transcutol (0.5 mL). Before adding CUR (30 mg) to the lipid phase and continuing to heat the bottle until a clear, homogenous solution formed, the phospholipids and CTAB were dissolved by heating it to a continuous 70 °C in a water bath. Following that, 9.5 ml of double-distilled water kept at 70°C was immediately poured into lipid phase with continuous mixing (1200 rpm) until a uniform nano dispersion was created[23].

Optimization of CUR– LP by custom design Model

Optimization was done by using a custom design, using Design Expert® software (version 13.0, Stat-Ease Inc., Minneapolis, USA). While EE (Y1), particle size (Y2), and PDI (Y3) were chosen as dependent factors, soylecithin (A) and CTAB (B) were chosen as independent variables (Table 1). CUR-LP formulations were created, and the responses of each CUR-LP were applied to various experimental models (linear, 2F, quadratic, and cubic) in order to analyse the best-fit model. The results confirmed using the ANOVA test. A polynomial equation, a contour plot, and a (3D) graph were computed for entrapment efficiency and PDI, particle size.

Evaluation of CUR-LP

Particle size and Polydispersity index

CUR-LP particle size and PDI were analyzed using photon correlation spectroscopy at 25.1 °C with a 90° detection angle. Double-distilled water, passed through a 0.45 µm filter, was utilised for diluting samples and maintain ideal light scattering conditions.

Entrapment efficiency

Encapsulation efficiency of the CUR-LP formulation was evaluated by adding 1000 mg of NaCl to 10 mL of the dispersion, centrifugation at 8,000 rpm for 60 min to promote phase separation. The supernatant was analysed spectrophotometrically at 425 nm to get concentration of free (un-encapsulated) curcumin, using a validated calibration curve ($R^2 = 0.999$). The (EE %) was measured using the following equation:

$EE\ (\%) = [(T - C)/T] \times 10$

where *T* is amount of curcumin used and *C* is amount of free curcumin[24]

Zeta potential

Zetasizer Delsa™ Nano (Beckman Coulter, Brea, USA) was used to evaluate the particle surface charge. The zeta potential, an essential parameter for assessing stability of nanoparticles, was measured using electrophoretic light scattering (Horiba SZ-100, Japan) at 25 °C, with 3.3 V voltage and a sample conductivity 0.394 mS/cm[25].

Differential scanning calorimetry (DSC)

Differential scanning calorimetry was conducted to know effect of temperature on curcumin-loaded LeciPlex using a Perkin Elmer 4000 instrument (Germany). 3–4 mg of the sample was subjected to thermal analysis, with temperature increased from 20 °C to 420 °C at a constant heating rate[26].

SEM

The outer structure of curcumin-loaded LeciPlex was examined using Scanning Electron Microscopy (SEM) at (Icon labs, Mumbai). A small amount of the dried leciplex were placed on a carbon tape and wrapped with gold to follow conductivity. The sample was then observed under the SEM at 20.0 kV with a magnification of 16000x.

Preparation of Hydrogel containing CUR-LP

To prepare the gel, Carbopol 940 was initially distributed in water and allowed to swell overnight. Neutralization was carried out using triethanolamine. Magnetic stirrer was utilized for formation of uniform blend of CUR-LP into gel. All constituents were combined in calculated ratios to formulate uniform gel, containing 0.035% (w/w) curcumin.

Evaluation of Hydrogel containing CUR-LP

Appearance, Clarity and pH

The clarity of the developed formulation before and after gelation was evaluated using white and black background to determine the appearance and clarity of the formulation. Additionally, the pH of the formulation was measured by digital pH meter (EQ-610, Equip Tronics, and Mumbai, India)[27].

Rheological studies

Gel viscosity was determined at ambient temperature (around 25 °C) using a Brookfield viscometer fitted with spindle no. 64, operating at 100 rpm. About 100 mL of the gel was transferred into a beaker for the measurement. The viscosity was recorded in centipoise (cP)[28].

Determination of spreadability

Parallel plate method was used for spreadability. Around 0.1 g of the formulation was positioned within a 0.5 cm radius circle noted on a glass slide. Another

slide was carefully placed over it, followed by the application of a 200 g weight for 5 minutes. The spread diameter was then measured to determine the extent of gel spreading[29].

Texture analysis

The mechanical possession of hydrogels was tested using a texture-Pro CT V1.3 texture analyser (Brookfield Engineering Labs) with a 10Kg load cell and a TA3/100 probe. The probe compressed each sample twice at 0.5 mm/s to a depth of 10 mm, with a 15 s interval between compressions. Measurements were done in triplicate at room temperature (~21 ± 2 °C). Texture Exponent software was used to evaluate hardness, adhesiveness from force–time graphs. [30].

In vitro drug release study

Franz diffusion cell with capacity of 20 mL and a diffusion area of 2.08 cm² was used to study *in vitro* drug release. A dialysis membrane separated the donor and receptor chambers. CUR-LPG was evenly applied to the membrane. The receptor side contained pH 6.8 buffer, stirred continuously at 37 ± 0.5 °C. To preserve sink conditions, 1 mL samples were drawn and filled back with fresh media. The collected aliquots were appropriately diluted and read spectrophotometrically to determine amount of CUR released over period. The release of CUR-LPG was assimilated with that of a commercial curcumin cream (1% w/w) and CUR-LP[31].

EX-vivo permeation study

These studies executed using Franz diffusion apparatus with receptor volume of 20 mL, area of 2.08 cm². Freshly excised goat skin, obtained from a local slaughterhouse, was employed as the biological membrane. The CUR-LPG formulation was loaded to the donor compartment, while the receptor chamber was filled with PBS (pH 6.8) and replicate physiological condition. The skin was placed between the two chambers. At specific time intervals, samples were extracted, suitably diluted, and assessed at 425 nm using a spectrophotometrically to determine curcumin concentration. From the resulting data, parameters such as cumulative drug permeation (Q_{42}, µg/cm²) and the permeability coefficient (Kp, cm/h) were calculated[32].

Antifungal study

The antifungal activity of CUR-LPG evaluated using the agar well diffusion method against *Candida albicans*. To fix the agar medium, essential components were dissolved in distilled water and subsequently sterilized using an autoclave at 15 psi and 121 °C for 20 minutes. Post-sterilization, the medium was transferred into sterile Petri dishes and left undisturbed at r 37 °C to solidify, after the agar solidified, a consistent layer of *Candida albicans* was uniformly applied over the surface. Using a sterile stainless-steel borer, wells punched into the medium, and each was filled with either the CUR-LPG formulation or a placebo using a sterile syringe. The inoculated plates nurtured at a temperature range of 28–35 °C for 48 hours to facilitate fungal proliferation. Upon completion of the incubation period, the diameters of the inhibition zones around each well were recorded to evaluate the antifungal activity[33].

RESULTS

Pre-formulation studies

Solubility study

Solubility was evaluated in various solvents, and the results were revealed in Table No. 01. Curcumin exhibited extremely low solubility in water, with a measured value of 0.0016 mg/mL, indicating its poor aqueous solubility. In contrast, a significantly higher solubility was observed in ethanol (13 mg/mL), suggesting ethanol as a suitable solvent for enhancing curcumin's solubility. At 0.0059 mg/mL, curcumin demonstrated marginally greater solubility than water in PBS, pH 6.8. These results emphasize curcumin's hydrophobic properties and provide credence to the use of organic solvents or formulation techniques to increase its bioavailability.

Table 1: Solubility of curcumin in different solvents.

Drug	Solubility in water (mg/ml)	Solubility in ethanol (mg/ml)	Solubility in PBS (6.8) (mg/ml)
Curcumin	0.0016	13	0.0059

Standard curve of curcumin in ethanol

A standard curve for curcumin in ethanol was constructed in range of 1–9 µg/mL and the linear regression equation, $y = 0.099x + 0.0475$, with a (R^2) of 0.9993, demonstrating excellent linearity. The corresponding linearity plot is presented in Figure 1a.

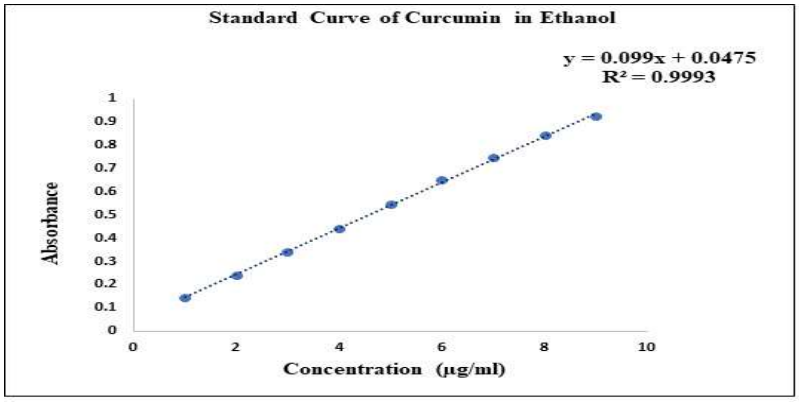

Figure 1a: Linearity plot of curcumin in ethanol

Standard curve of Curcumin in phosphate buffer (PBS) 6.8

A curcumin calibration curve has been created for the concentration range of 0.5–5 µg/mL in PBS, pH 6.8. Excellent linearity was indicated by (R2) of 0.9993 and the equation y = 0.174x + 0.0299 that was obtained from the data (Figure 1b). This robust association demonstrates that, within the investigated concentration range, the absorbance obeyed Beer-Lambert's rule. Figure (1b) illustrates the calibration curve's linearity, confirming the technique for precise curcumin quantification in PBS.

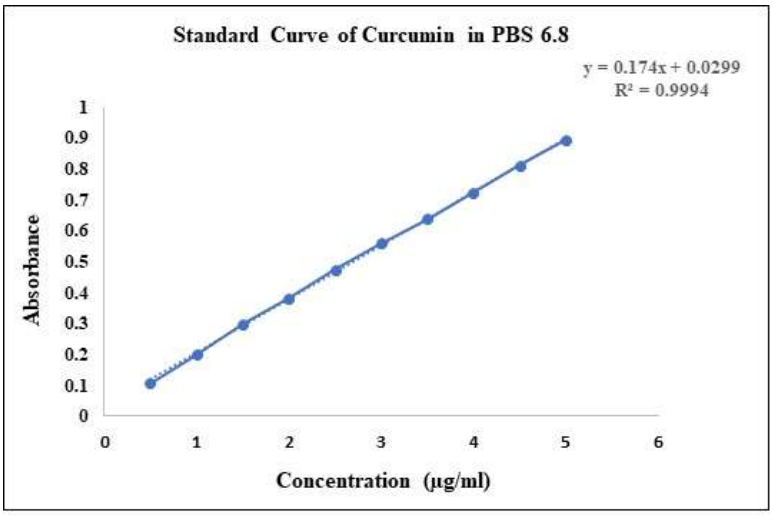

Figure 1b: linearity plot of curcumin in PBS 6.8

FTIR analysis

The FTIR spectrum of the curcumin drug sample was analyzed to identify characteristic functional groups (Figure 1c). A broad band around 3222 cm^{-1} indicated O–H stretching, confirming phenolic hydroxyl groups. A sharp peak at approximately 738 cm^{-1} corresponded to C–H bending vibrations, arising from both aromatic and aliphatic hydrogen atoms. A prominent peak near 1681 cm^{-1} was assigned C=O stretching confirmed a conjugated diketone; peaks near 1560 cm^{-1} indicated aromatic C=C stretching. Supporting the existence of benzene moieties. Additional bending vibrations of C–H bonds were noted in the 1450–1350 cm^{-1} region. These spectral features collectively confirm the chemical structure of curcumin.

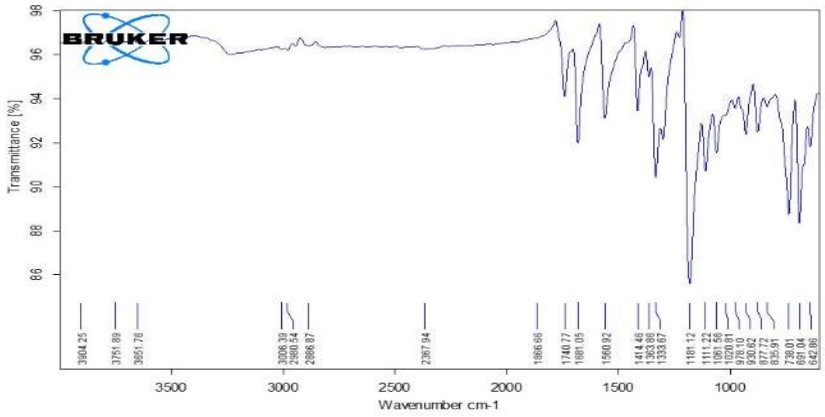

Figure 1c: FTIR spectra of Curcumin (Drug).

FTIR of Cetyltrimethylammonium Bromide (CTAB)

The FTIR of CTAB was recorded and characteristic peaks were observed at Peaks at 2914 cm^{-1} and 1461 cm^{-1} indicated C–H stretching and bending; 960 cm^{-1} confirmed C–N stretching, verifying CTAB's quaternary ammonium group and structural integrity (Figure 1d).

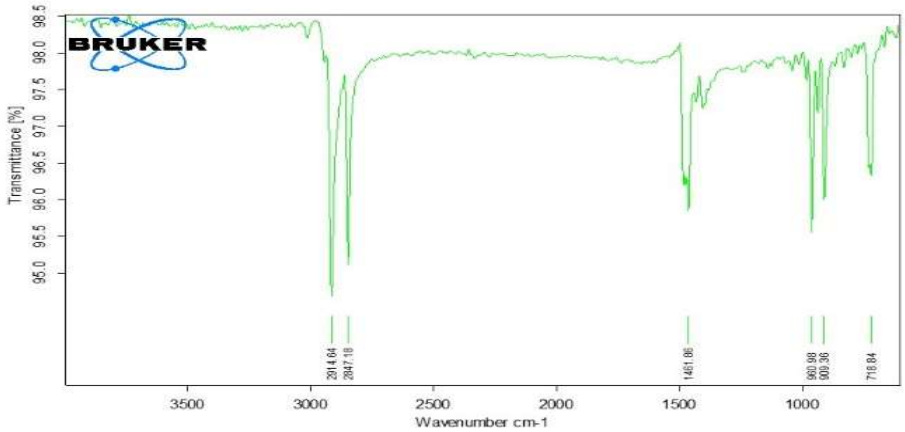

Figure 1d. FTIR spectra of Cetyltrimethylammonium Bromide (CTAB).

FTIR Analysis of Transcutol

The Fourier Transform Infrared (FTIR) spectrum of Transcutol HP was recorded to confirm its chemical identity and assess the presence of functional groups (Figure 1e). Peak at 3437 cm^{-1} indicated O–H stretching; 2926 cm^{-1}, C–H stretching; 1106 cm^{-1}, C–O–C stretching, confirming alcohol and ether group in transcutol HP, consistent with its chemical structure as diethylene glycol monoethyl ether. The results validate its structural integrity and suitability for use as a solubilizer and permeation enhancer in pharmaceutical formulations.

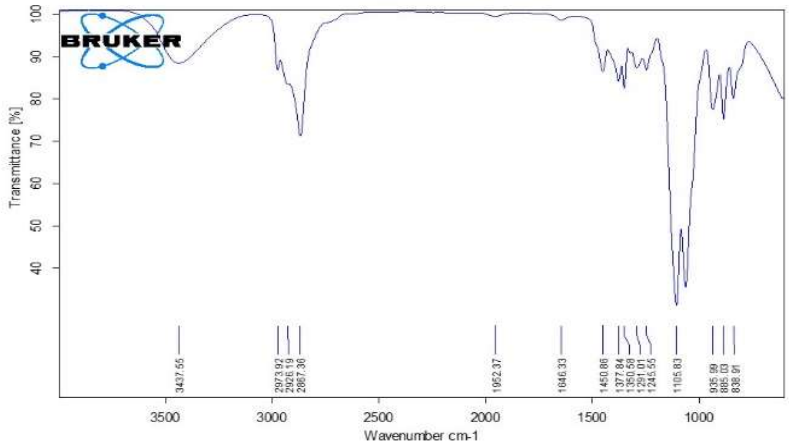

Figure 1e: FTIR spectra of Transcutol HP.

FTIR of physical mixture

The FTIR of physical mixture (Figure 1f), was analyzed to investigate any possible chemical interactions among the components. The spectrum revealed distinct absorption bands corresponding to the functional groups of the individual constituents, indicating that their chemical structures remained unchanged within the mixture. Prominent peaks were detected around 3350 cm^{-1} (O–H signaling), 2920–2850 cm^{-1} (C–H signaling), 1735 cm^{-1} (C=O signaling), and within the range of 1050–1250 cm^{-1} (C–O signaling). The lack of noticeable peak shifts, disappearance, or formation of new bands suggests that no significant chemical interactions occurred, thereby confirming the compatibility of the components in the physical blend.

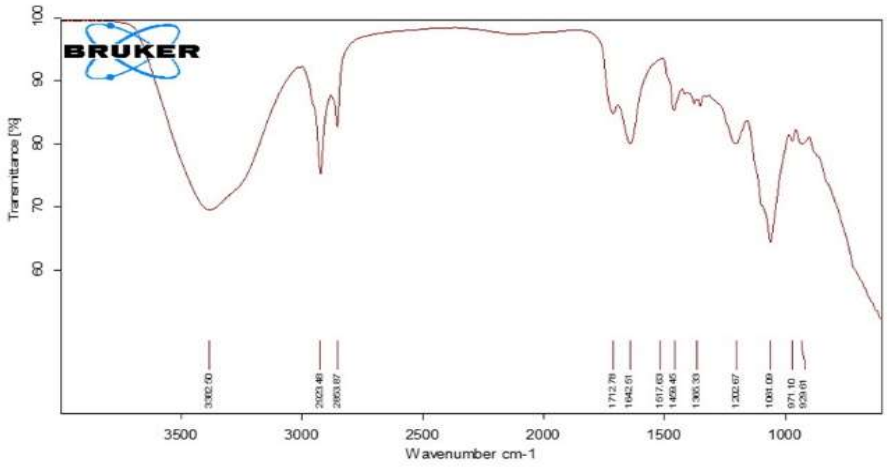

Figure 1f: FTIR spectra of Physical mixture.

FTIR overlay spectrum

The FTIR overlay spectrum illustrates the characteristic functional group vibrations of Curcumin, CTAB (Cetyltrimethylammonium bromide), and Transcutol, confirming their chemical identities and interactions in the formulation. For Curcumin, notable peaks include O–H stretching at 3222 cm^{-1}, C=O stretching at 1681 cm^{-1}, and aromatic C=C stretching at 1560 cm^{-1}, indicating phenolic and conjugated diketone functionalities. CTAB shows distinct C–H stretching and bending at 2914 cm^{-1} and 1461 cm^{-1}, respectively, corresponding to its long hydrocarbon chain (Figure 1g). Transcutol presents C–H deformation at 1377 cm^{-1} and C–H rocking/wagging 986 cm^{-1}, affirming its presence as a solvent/co-solvent.

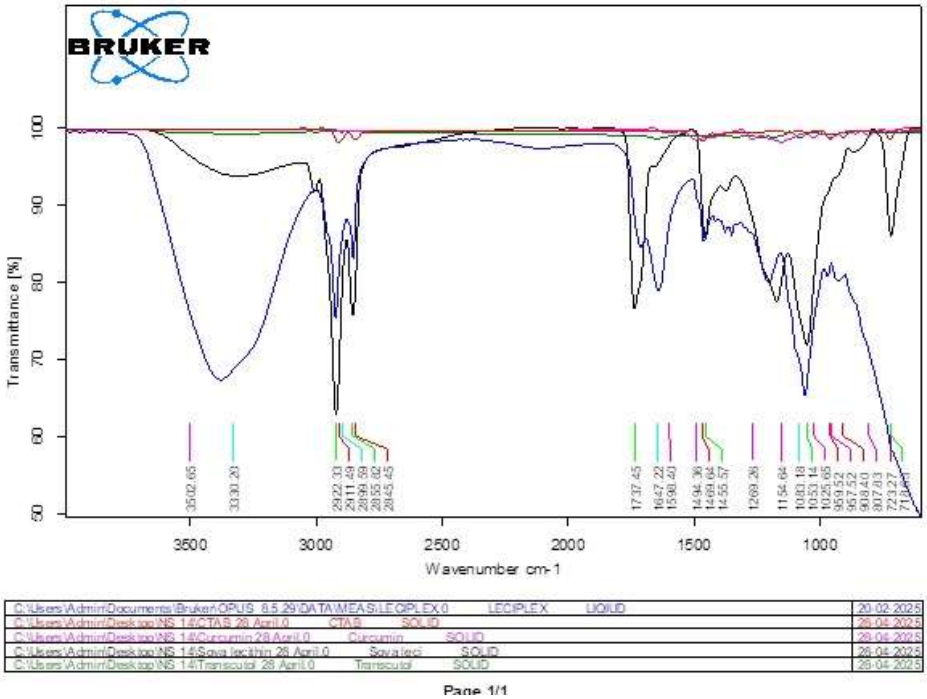

Figure 1g: FTIR Overly Spectrum

Optimization of CUR-LP by Custom Design

Optimization of CUR – LPG was done using a response surface method custom design, to evaluate two independent variables— concentrations of surfactant, phospholipid—on the aforementioned response parameters. Nine experimental formulations were developed to statistically assess these effects. Optimized CUR–LP formulation comprised curcumin (30mg) phospholipid (175 mg), CTAB (105 mg), Transcutol P (0.5 mL), and distilled water (9.5 mL).

Impact of Independent Variables on Entrapment Efficiency (EE %)

EE across different formulations lie in 86.9% to 98.54%, as shown in Table 2. Statistical analysis indicated that the quadratic model was highly significant, demonstrated by F-value (4.69) and p-value (< 0.0001). Additionally, the sequential p-value (0.0035) supports the model's reliability. Adjusted and predicted R^2 values aligned well, and a precision value of 6.432 confirmed the model's suitability for design optimization.

$Y=69.82+0.178A+0.381B-0.000837AB-0.000376A^2-0.00165B^2$(4)

The coefficients for A (soyalecithin) and B (CTAB) suggest that elevation in concentrations leads to higher entrapment efficiency, likely due to enhanced vesicle formation and stabilization. However, the negative quadratic terms imply that excessively high levels of these components can reduce EE%, possibly due to vesicle instability or saturation. The corresponding 3D surface plot (Figure 2) further supports the selection of a quadratic model for optimizing EE%.

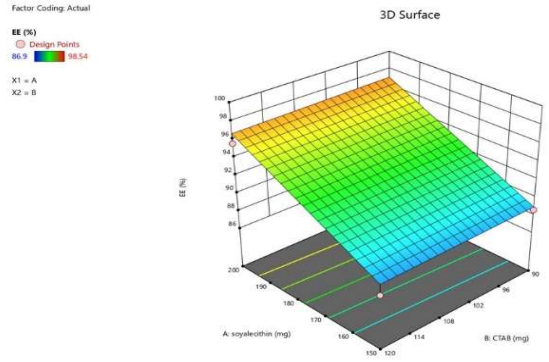

Figure 2: 3D surface plot demonstrates the effect of an independent variable on Entrapment efficiency

Impact of Independent Variables on Particle Size

The measured particle size for different formulation batches ranged from 186 nm to 349 nm, as shown in Table 2. The developed quadratic model was found to be statistically significant, with F-value (4.61) ($p < 0.0001$) and a sequential p-value (0.0050), confirming reliability. The predicted and adjusted R^2 values were in good agreement, and an adequate precision of 6.468 indicated a desirable signal-to-noise ratio, supporting the model's use in optimizing particle size within the experimental space.

$$Y=428+4.30A+11.45B-28.46AB-10.84A^2-2.90B^2 \quad (5)$$

The positive coefficients for A (soyalecithin) and B (CTAB) suggest that an increase in either component rises particle size. This confirms formation of larger vesicles as more lipid or surfactant material becomes available for vesicle assembly. The negative coefficients of AB, A^2, and B^2 indicate that beyond certain levels, interactions between the components or excessive concentrations may lead to a reduction in particle size, likely due to changes in vesicle stability or packing efficiency. The corresponding 3D surface plot (Figure 3) further confirms that the quadratic model offers good suits to data. This used to predict particle size behavior effectively, based on variations in soyalecithin and CTAB concentrations.

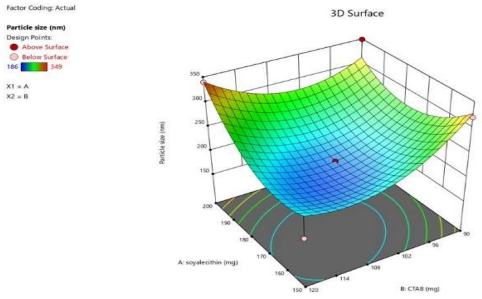

Figure 3: Three -dimensional surface plot demonstrate the effect of independent variables on Particle size

Impact of Independent Variables on Polydispersity Index (PDI)

The PDI values ranged between 0.352 and 0.595 (Table 2), indicating moderate homogeneity in particle size distribution. The quadratic model developed for PDI was statistically relevant to F-value 7.03 ($p = 0.0117$), and p-value of 0.0394 confirmed importance of the model. Although the predicted R^2 was slightly negative (-0.18), adjusted R^2 (0.715) and adequate precision value of 6.03 support the model's relevance for design space evaluation.

$$Y=0.418+0.0309A-0.0254B+0.0608AB+0.0731A^2+0.0486B^2 \quad (6)$$

The positive coefficient for A (soyalecithin) indicates that increasing its concentration may lead to a slight rise in PDI, possibly due to the formation of varied vesicle sizes. In contrast, the negative coefficient for B (CTAB) implies that higher surfactant levels can promote uniform particle formation, thereby lowering the PDI. The interaction (AB) and squared terms (A^2, B^2) further demonstrate the complexity of their effects. These trends are visually confirmed in the 3D surface plot (Figure 4), emphasizing that a quadratic model appropriately describes the PDI behavior.

C

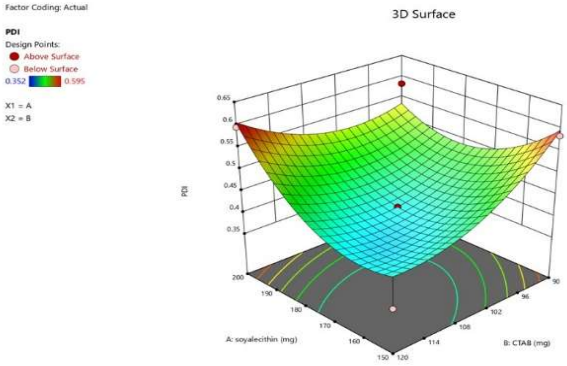

Figure 4: Three -dimensional surface plot demonstrate the effect of independent variables on PDI

*Author for Correspondence: Praful.pharma@gmail.com

Table 2: Custom design represents variable with their levels and measured responses from experimental runs

Run	Factor-1 A: Soya lecithin (mg)	Factor-2 B: CTAB (mg)	Response-1 EE (%)	Response-2 Particle Size (nm)	Response-3 PDI
1	150.0	120.0	87.4	186	0.352
2	175.0	105.0	92.8	206	0.418
3	210.3	105.0	98.54	313	0.577
4	139.6	105.0	86.9	309	0.574
5	200.0	90.0	96.24	349	0.583
6	150.0	90.0	88.6	320	0.583
7	175.0	126.2	94.8	306	0.532
8	200.0	120.0	95.6	340	0.595
9	175.0	83.78	94.5	301	0.521

Assessment and Characterization of CUR–LP Formulation

Particle Size, PDI, Entrapment Efficiency, and Zeta Potential

The optimized leciplex formulation of CUR was systematically evaluated. The mean particle size of the formulation was 206.6nm, confirming the formation of nano sized vesicles suitable for enhanced topical penetration. The Polydispersity index (PDI) was measured to be 0.418 ± 0.046.

The formulation exhibited entrapment efficiency (%EE) of 92.81 ± 1.02%, suggesting efficient incorporation of curcumin within the lipid bilayer structure. This high encapsulation may be attributed to the lipophilic nature of the drug and its strong interaction with the phospholipid and surfactant matrix.

The optimized batch exhibited zeta potential (+26.30 mV), which can be attributed to the incorporation of the cationic surfactant, Cetyltrimethylammonium bromide (CTAB). This positive surface charge contributes to electrostatic stabilization by minimizing particle aggregation, thereby enhancing the colloidal stability of the system (Figure 5). Moreover, the presence of positively charged vesicles is anticipated to promote electrostatic interactions with the negatively charged skin surface, which may enhance drug deposition and improve permeation across the stratum corneum.

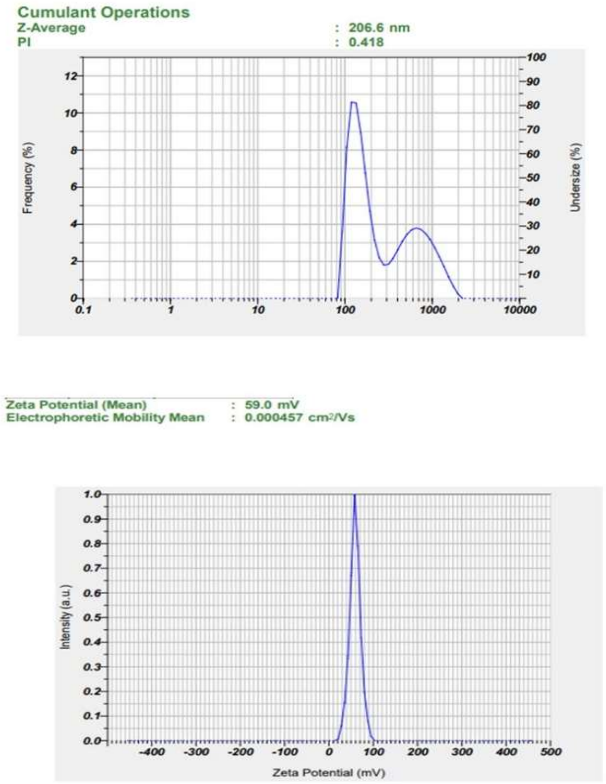

Figure 5. (a) Particle size and (b) Zeta potential of optimized batch

DSC study

The DSC study in (Figure 6) illustrates the thermal behaviour of pure curcumin (API) and the curcumin-loaded Leciplex (CUR-LP) formulation. Pure curcumin exhibits a distinct peak at 179.5 °C, conforming melting point and crystallinity. However, piercing peak

absent in DSC profile of CUR-LP formulation, suggesting that curcumin is no longer in its crystalline form. Instead, two broad thermal events appear around 123 °C, which may be attributed to the thermal properties of formulation excipients such as lecithin, CTAB, or the evaporation of Transcutol. The disappearance of the curcumin melting peak in the formulation indicates successful encapsulation and a likely transition of the drug into an amorphous or molecularly dispersed state within the nanocarrier. This change may enhance the solubility and bioavailability of curcumin.

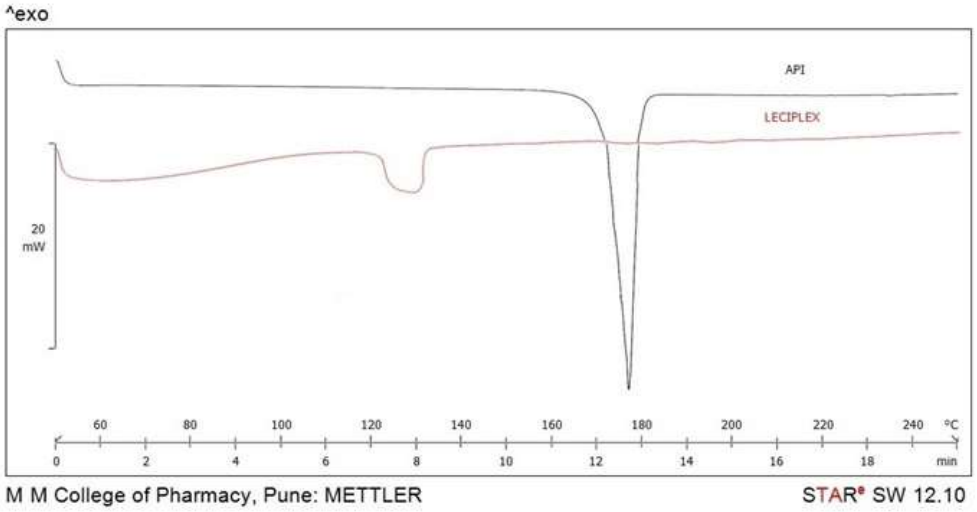

Figure 6: DSC thermogram of pure drug and CUR-LP

Scanning Electron Microscopy (SEM)

As shown in figure 7; demonstrates the formation of spherical to nearly spherical particles with relatively uniform distribution and no signs of aggregation, indicating good dispersion. The surface appears smooth, which may reflect successful encapsulation of the drug within the vesicular matrix. The nano scale size of the particles, as inferred from the scale bar (5.0 µm), supports their potential suitability for enhanced skin permeation and bioavailability.

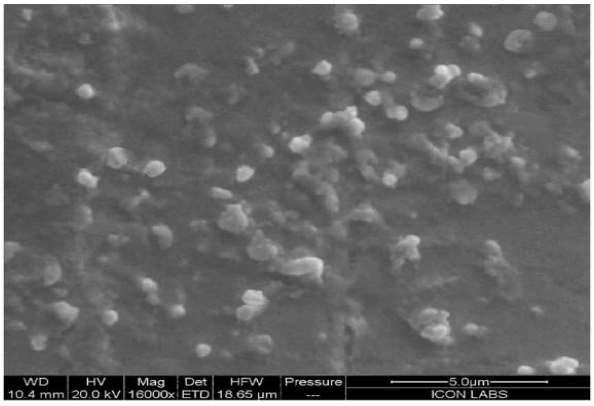

Figure 7: Scanning electron microscopy of leciplex

Assessment of CUR-LPG

Clarity, Visual characteristics and pH

The prepared curcumin gel exhibited a smooth, homogeneous texture with a uniform yellow colour and no visible lumps or grittiness. The formulation had a characteristic mild odour consistent with curcumin. The observed pH of the gel was 5.64 ± 0.1, which falls within the acceptable range of 5.5–6.5 for topical application, ensuring skin compatibility. The pH was adjusted using Triethanolamine (TEA), which neutralized the gelling agent to form a stable gel and maintain suitable pH.

Viscosity

The sample was placed in the viscometer container, and spindle No. 64 was used at a rotation speed of 100rpm to record the viscosity. The viscosity was found to be 5837 ± 146.22 cps.

Spreadability

Spreadability is a critical parameter influencing patient compliance, as it ensures easy and uniform application of the topical formulation. A well-spreadable gel enhances user comfort and therapeutic effectiveness. To evaluate the spreadability of the CUR–LPG formulation, the glass plate method was employed. The results showed that the gel exhibited a spreadability range of 5.8 to 6.5 cm, which falls within the

acceptable standard of 5 to 7 cm, indicating adequate and consistent spreadability. These findings confirm that the gel has a suitable consistency for topical application, ensuring smooth and effortless spreading over the skin.

Texture analysis

The textural properties of the CUR–LPG gel were evaluated to ensure its suitability for topical application (Figure 8). The gel exhibited a hardness of 45 g with a deformation value of 9.9 mm, indicating a balanced firmness that allows easy dispensing without leakage. The work cycle during hardness testing was 1.2mJ, reflecting the energy needed for extrusion and confirming smooth applicability. Adhesiveness was recorded as 1.2 mJ, suggesting adequate stickiness for localized retention without compromising spreadability. Additionally, the adhesive force was measured at 22 g, supporting the formulation's ability to maintain contact with the skin surface. These values collectively confirm that the gel possesses optimal mechanical strength and adhesive behavior, making it well-suited for effective and user-friendly topical delivery.

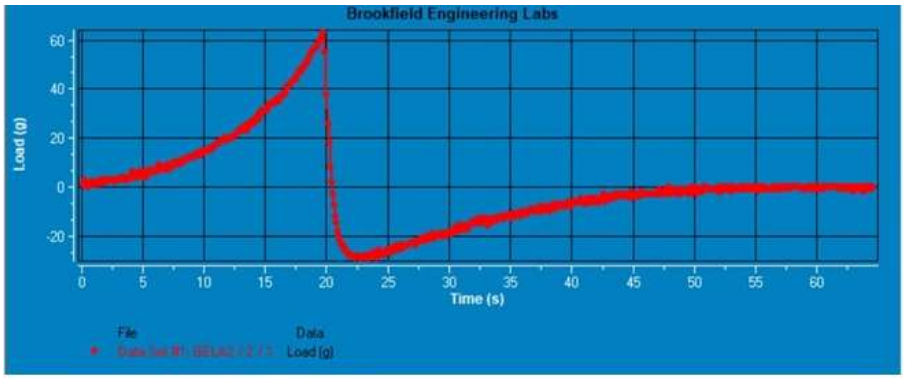

Figure 8: Texture analysis of CUR-LP

In-vitro analysis

The release of CUR from three formulations—CUR–LP, CUR–LPG, and a marketed product with results illustrated in Figure 9a. The marketed formulation exhibited fast release, 50% CUR released in the first 4 hours, reaching a cumulative release of 96.45 ± 1.3% at 8 hours. In contrast, the CUR–LP suspension exhibited a slower release profile, with less than 30% released in 4 hours and a total of 86.46 ± 2% at 8 hours. The CUR–LPG gel showed the most controlled release, with less than 20% released in 4 hours and a final cumulative release of 76.70 % at 8 hours. The reduced release rate in the LP and LPG formulations is attributed to the encapsulation of CUR within lipid structures and the viscous nature of the gel matrix, respectively. The sustained release behaviour of CUR–LPG suggests its potential to maintain therapeutic levels over an extended period.

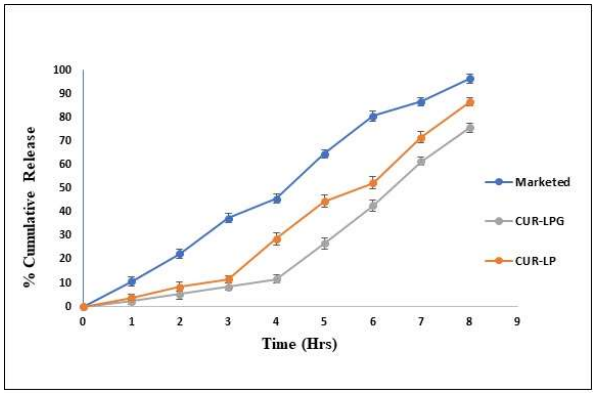

Figure 9a: In-vitro drug release data for CUR-LP, CUR-LPG and marketed formulation phosphate buffer solution pH 6.8 (n=3 ± SD)

Ex -vivo permeation study

This study performed using goat abdominal skin to compare CUR permeation profiles of the marketed curcumin formulation and the CUR–LPG. The permeation of curcumin per unit area was measured over an 8-hour period. The marketed formulation showed a higher cumulative permeation of 93.95 ± 0.8%, while the CUR–LPG gel demonstrated a slower permeation of 74.61 ± 0.3 % (Figure 9b). The lower permeation rate from CUR–LPG can be attributed to the viscous gel matrix, which created a diffusion barrier, resulting in a sustained and controlled release profile. The

difference in permeation between CUR–LPG and the marketed product notable ($p < 0.05$), indicating that CUR–LPG system effectively modulates curcumin release, potentially enhancing its therapeutic efficacy over an extended duration.

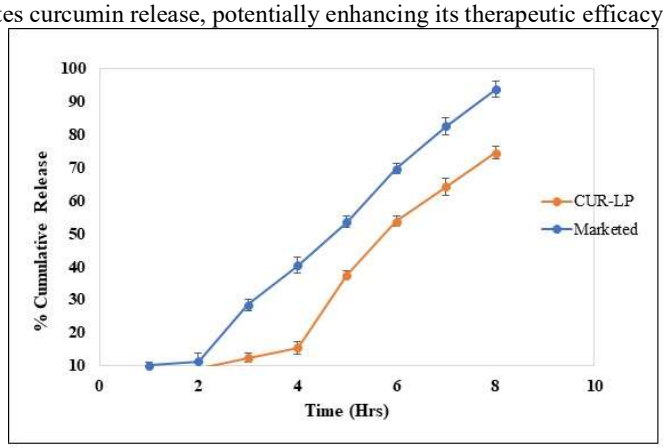

Figure 9b: *EX-vivo* permeation profile of CUR-LP and marketed formulation using goat skin.

Antifungal assay

To evaluate the therapeutic potential of CUR–LP and CUR–LPG formulations against fungal infections, an antifungal study was conducted using Candida albicans as the test organism. This method has been widely reported in literature for assessing antifungal activity through ZOI measurement.

After 48 hours of incubation, the results (Table 3) revealed that curcumin-loaded Leciplex (CUR–LP) exhibited improved antifungal action compared to the marketed curcumin formulation, likely due to enhanced drug penetration facilitated by the cationic liposomal system. Furthermore, the CUR–LPG formulation demonstrated an even greater and prolonged antifungal effect. This sustained activity is attributed to the viscous gel matrix, which modulates drug release and maintains therapeutic levels over time by slowing diffusion through the gel structure (Figure 10). These findings support the enhanced antifungal potential of CUR–LPG for topical application.

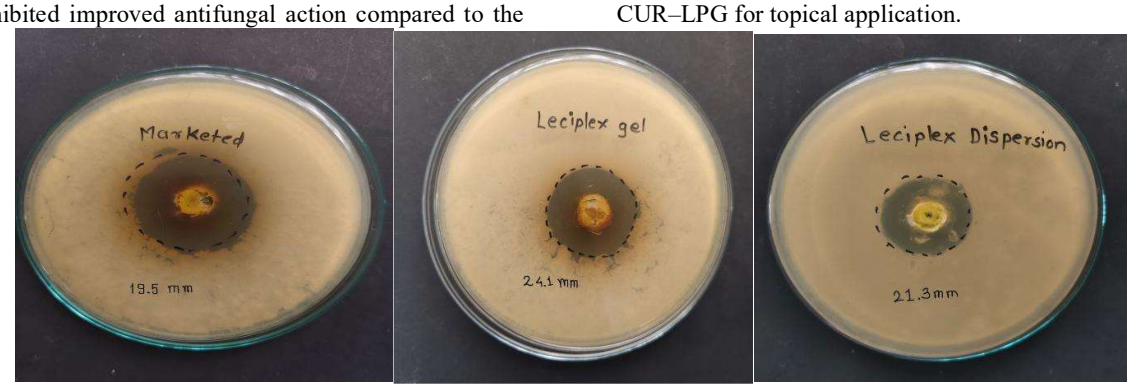

a **b** **c**

Figure 10: Anticandidal action of (a) Marketed (b) CUR-LPG and (c) CUR-LP

Table 3: Zone of Inhibition of Various Formulations against Candida *albicans*

Sr.no	Formulation	Zone of inhibition (mm)
1	CUR-LP	21.3 ± 0.8
2	CUR-LPG	24.1 ± 0.6
3	Marketed	19.5 ± 1.0

Discussion

This study focused on developing a curcumin-loaded Leciplex (CUR–LP) system and its gel-based formulation (CUR–LPG) to enhance the topical treatment of candidiasis. Curcumin's therapeutic applications have long been limited by its low solubility and poor bioavailability. By incorporating curcumin into lipid-based nanocarriers, the study aimed to overcome these drawbacks and improve both drug delivery and efficacy.

The optimized CUR–LP formulation demonstrated desirable physicochemical characteristics, including a small particle size (~206.6 nm) and a narrow particle size distribution (PDI 0.418), supporting uniformity and stability. High entrapment efficiency (92.81 ± 1.02%) indicated successful incorporation of curcumin into the lipid matrix, which can be attributed to its lipophilic nature and interaction with phospholipids and surfactants. The positive zeta potential (+26.30 mV), due to the presence of CTAB, enhances stability and supports better adhesion to the

negatively charged skin surface, facilitating deeper penetration.

Thermal analysis using DSC confirmed that curcumin was effectively incorporated in an amorphous or dispersed form, as indicated by the disappearance of its characteristic melting point. SEM imaging further validated the formation of uniformly distributed, spherical nanoparticles, consistent with nanoscale morphology.

Incorporation of CUR–LP into a Carbopol 940 gel matrix resulted in a formulation (CUR–LPG) with favourable characteristics for topical use. The gel was smooth, uniform, and had a skin-compatible pH (5.64 ± 0.1). Rheological and textural evaluations revealed that the formulation was easy to apply, spreadable, and had good mechanical strength, which are essential for patient comfort and consistent drug application.

The in vitro release study highlighted the sustained-release nature of the CUR–LPG gel compared to CUR–LP and a commercially available curcumin cream. This controlled release can be attributed to both the lipid carrier system and the gel matrix, which together create a diffusion barrier and prolong drug availability at the site of application. Similarly, ex vivo permeation studies showed that the gel formulation resulted in slower but steady drug permeation through the skin, suggesting improved retention and localized drug action.

In terms of antifungal activity, both CUR–LP and CUR–LPG formulations demonstrated greater effectiveness against *Candida albicans* than the marketed product. CUR–LPG exhibited the largest zone of inhibition (24.1 ± 0.6 mm), indicating enhanced bioavailability and sustained action due to its formulation. This confirms the benefit of combining a cationic nano-carrier with a hydrogel base for prolonged and targeted topical antifungal therapy.

Conclusion

This study successfully developed and optimized a CUR–LP formulation using Custom Design, achieving high drug entrapment efficiency (~92.8%) with uniform nano sized particles (~204 nm, PDI 0.418), indicating good stability. The CUR–LP was effectively incorporated into a Carbopol gel base to form CUR–LPG, which was then characterized for its spreadability, pH, viscosity, , texture all of which confirmed its suitability for topical application.

Drug release studies, in vitro and ex vivo, showed that CUR–LPG formulation offered sustained release, enhancing curcumin retention on the skin over time. The antifungal activity assessed against *Candida albicans* demonstrated that both CUR–LP and CUR–LPG provided superior antifungal effects compared to a conventional marketed formulation.

Overall, the results support the potential of CUR–LPG as a promising and effective topical therapy for fungal infections, offering enhanced stability, extended drug release, and improved therapeutic efficacy.

Abbreviation-

CTAB: Cetyl trimethyl ammonium bromide
DSC: Differential Scanning Calorimetry
EE: Entrapment Efficiency
LP: Leciplex
CUR-LP: Curcumin loaded leciplex
CUR-LPG: Curcumin loaded leciplex gel
NM: Nanometre
PDI: Polydispersity index
PS: Particle size
RPM: Rotation per minute

Acknowledgements:
Authors thankful to Herbo Nutra Pvt. Ltd (India) for providing Curcumin and Lubrizol I Private Limited, (Mumbai) for providing Carbopol 940.

Contribution of Authors: Dr. Prafulla S. Chaudhari, Nikita Shinde., Dr. Priyanka Chaudhari Dr. Ashlesha Pandit, Dr Rohini Kolhe and Dr Manisha Khaire contributed to the design and implementation of the research, to the analysis of the results and to the writing of the manuscript.

Ethics approval and consent to participate: Not applicable

Declaration of interest statement: All authors have read and approved the final version of the manuscript and there are no conflicts of interest to declare.

Competing interests: The authors declare that they have no competing interest.

References:

1. Denning DW. Global incidence and mortality of severe fungal disease. *Lancet Infect Dis* 2024; 24: e428–e438. 20240112. DOI: 10.1016/s1473-3099(23)00692-8.
2. Tarannum N, Pooja K, Jakhar S, et al. Nanoparticles assisted intra and transdermic delivery of antifungal ointment: an updated review. *Discover Nano* 2024; 19: 11. 20240109. DOI: 10.1186/s11671-023-03932-3
3. Niño-Vega GA, Padró-Villegas L and López-Romero E. New Ground in Antifungal Discovery and Therapy for Invasive Fungal Infections: Innovations, Challenges, and Future Directions. *Journal of Fungi* 2024; 10: 871.
4. Urosevic M ea. Curcumin: Biological Activities and Modern Pharmaceutical Forms. *Antibiotics* 2022; 11: 135. DOI: 10.3390/antibiotics11020135
5. Toden S and Goel A. The Holy Grail of Curcumin and its Efficacy in Various Diseases: Is Bioavailability Truly a Big Concern? *J Restor Med* 2017; 6: 27–36. DOI: 10.14200/jrm.2017.6.0101.
6. Naksuriya O, Okonogi S, Schiffelers RM, et al. Curcumin nanoformulations: a

review of pharmaceutical properties and preclinical studies and clinical data related to cancer treatment. *Biomaterials* 2014; 35: 3365–3383. 20140115. DOI: 10.1016/j.biomaterials.2013.12.090.

7. Kunnumakkara AB, Bordoloi D, Padmavathi G, et al. Curcumin, the golden nutraceutical: multitargeting for multiple chronic diseases. *Br J Pharmacol* 2017; 174: 1325–1348. 20161021. DOI: 10.1111/bph.13621.

8. Wang R, Zou L, Yi Z, et al. PLGA nanoparticles loaded with curcumin produced luminescence for cell bioimaging. *Int J Pharm* 2023; 639: 122944. 20230410. DOI: 10.1016/j.ijpharm.2023.122944.

9. Halbandge SD, Jadhav AK, Jangid PM, et al. Molecular targets of biofabricated silver nanoparticles in Candida albicans. *J Antibiot (Tokyo)* 2019; 72: 640–644. 20190424. DOI: 10.1038/s41429-019-0185-9.

10. Metselaar JM and T. L. Challenges in nanomedicine clinical translation. *Drug Deliv Transl Res* 2020; 10: 721–725. DOI: 10.1007/s13346-020-00740-5.

11. Carita AC, Eloy JO, Chorilli M, et al. Recent Advances and Perspectives in Liposomes for Cutaneous Drug Delivery. *Curr Med Chem* 2018; 25: 606–635. DOI: 10.2174/0929867324666171009120154.

12. Date AA, Srivastava D, Nagarsenker MS, et al. Lecithin-based novel cationic nanocarriers (LeciPlex) I: fabrication, characterization and evaluation. *Nanomedicine (Lond)* 2011; 6: 1309–1325. DOI: 10.2217/nnm.11.38.

13. Shah SM, Ashtikar M, Jain AS, et al. LeciPlex, invasomes, and liposomes: A skin penetration study. *Int J Pharm* 2015; 490: 391–403. 20150519. DOI: 10.1016/j.ijpharm.2015.05.042.

14. Wei L ea. Recent Progress in Hydrogel Synthesis and Biomedical Applications. *Gels* 2025; 11: 456. DOI: 10.1021/acsapm.2c00482

15. Zondlo Fiume M. Final report on the safety assessment of Acrylates Copolymer and 33 related cosmetic ingredients. *Int J Toxicol* 2002; 21 Suppl 3: 1–50. DOI: 10.1080/10915810290169800.

16. Wei L ea. Substrate-Independent, Mechanically Tunable, and Scalable Gelatin Methacryloyl Hydrogel Coating with Drag-Reducing and Anti-Freezing Properties. *ACS Appl Polym Mater* 2022; 4. DOI: 10.1021/acsapm.2c00482.

17. Singh VK, Anis A, Banerjee I, et al. Preparation and characterization of novel carbopol based bigels for topical delivery of metronidazole for the treatment of bacterial vaginosis. *Mater Sci Eng C Mater Biol Appl* 2014; 44: 151–158. 20140812. DOI: 10.1016/j.msec.2014.08.026.

18. Tang C, Yin L, Yu J, et al. Swelling behavior and biocompatibility of Carbopol-containing superporous hydrogel composites. *Journal of Applied Polymer Science* 2007; 104: 2785–2791. DOI: 10.1002/app.25930.

19. Wang W, Narain R and H. Z. Hydrogels. 2020, pp.203–244.

20. Van Nong H, Hung LX, Thang PN, et al. Fabrication and vibration characterization of curcumin extracted from turmeric (Curcuma longa) rhizomes of the northern Vietnam. *Springerplus* 2016; 5: 1147. 20160722. DOI: 10.1186/s40064-016-2812-2.

21. Rapalli VK, Kaul V, Gorantla S, et al. UV Spectrophotometric method for characterization of curcumin loaded nanostructured lipid nanocarriers in simulated conditions: Method development, in-vitro and ex-vivo applications in topical delivery. *Spectrochim Acta A Mol Biomol Spectrosc* 2020; 224: 117392. 20190715. DOI: 10.1016/j.saa.2019.117392.

22. Boscariol R, Paulino TH, Oliveira Jr JM, et al. Characterization of Commercially Available Turmeric for Use in Pharmaceutical Products and Food Supplements. *J Braz Chem Soc* 2022; 33. DOI: 10.21577/0103-5053.20220073.

23. Caddeo C ea. Nanocarriers for antioxidant resveratrol: Formulation approach, vesicle self-assembly and stability evaluation. *Colloids Surf B Biointerfaces* 2013; 111C: 327–332. DOI: 10.1016/j.colsurfb.2013.06.016.

24. Salama A, Badran M, Elmowafy M, et al. Spironolactone-Loaded LeciPlexes as Potential Topical Delivery Systems for Female Acne: In Vitro Appraisal and Ex Vivo

Skin Permeability Studies. *Pharmaceutics* 2019; 12 20191225. DOI: 10.3390/pharmaceutics12010025.
25. Arozal W, Louisa M, Rahmat D, et al. Development, Characterization and Pharmacokinetic Profile of Chitosan-Sodium Tripolyphosphate Nanoparticles Based Drug Delivery Systems for Curcumin. *Adv Pharm Bull* 2021; 11: 77–85. 20201107. DOI: 10.34172/apb.2021.008.
26. Kumbhar S, Khairate R, Bhatia M, et al. Evaluation of curcumin-loaded chitosan nanoparticles for wound healing activity. *ADMET and DMPK* 2023; 11: 601–613. DOI: 10.5599/admet.1897.
27. M. Kmkm A and M. Ghareeb M. Formulation and In vitro Evaluation of Peppermint Oil Based Nanoemulgel of Luliconazole for Topical Application. *History of Medicine* 2023; 9.
28. Patel NA, Patel NJ and Patel RP. Formulation and evaluation of curcumin gel for topical application. *Pharm Dev Technol* 2009; 14: 80–89. DOI: 10.1080/10837450802409438.
29. Rajinikanth PS and J. C. Development and evaluation of nanostructured lipid carrier-based hydrogel for topical delivery of 5-fluorouracil. *Int J Nanomedicine* 2016; 11: 5067–5077. 20161005. DOI: 10.2147/IJN.S117511.
30. Vlad RA ea. Hydroxypropyl Methylcellulose-A Key Excipient in Pharmaceutical Drug Delivery Systems. *Pharmaceutics* 2025; 17 20250616. DOI: 10.3390/pharmaceutics17060784.
31. Patel NA, Patel NJ and RP. P. Formulation and evaluation of curcumin gel for topical application. *Pharm Dev Technol* 2009; 14: 80–89. DOI: 10.1080/10837450802409438.
32. Jacob S, Kather FS, BodduS HS, et al. Vesicular Carriers for Phytochemical Delivery: A Comprehensive Review of Techniques and Applications. *Pharmaceutics* 2025; 17 20250402. DOI: 10.3390/pharmaceutics17040464.
33. Bairagi G PV. Formulation and development of curcumin based emulgel in treatment and recurrence of vaginal candidiasis. *Int J Curr Pharm Res* 2021; 13(1): 89–99. DOI: 10.22159/ijcpr.2021v13i5.1900.